

A Versatile Nanoagent for Multimodal Imaging-Guided Photothermal Cancer Therapy and Anti-Inflammation

Ping Yan^a, Xian Shu^a, Pei-Ling Chen^b, Hao Zhong^b, Hai-Yan Gong^a, Shi-Song Han^c, Ying-Feng Tu^b, Xintao Shuai^d, Jie Li^{*a}, Li-Han Liu^{*b}, Ping Wang^{*a}

a. Department of Ultrasonography, The Third Affiliated Hospital of Southern Medical University, Academy of Orthopedics, Guangdong Province, Guangzhou 510515, P. R. China;

b. School of Pharmaceutical Sciences, Guangdong Key Laboratory of New Drug Screening, Southern Medical University, Guangzhou 510515, P. R. China.

c. Laboratory of Interventional Radiology, Department of Minimally Invasive Interventional Radiology, and Department of Radiology, the Second Affiliated Hospital of Guangzhou Medical University, Guangzhou, 510260, China.

d. PCFM Lab of Ministry of Education, School of Materials Science and Engineering, Sun Yat-sen University, Guangzhou 510275, China

Corresponding authors:

164757254@qq.com (Jie Li)

liulihan@smu.edu.cn (LihanLiu)

wangping3915@sohu.com (PingWang)

Content

Figure S1. Standard absorption curve of Celecoxib by UV-vis spectrophotometry.

Figure S2. The release curves of Celecoxib from T-lipos-CPAuNCs with/without laser irradiation (pH 6.5).

Figure S3. ^1H NMR spectra of Celecoxib pre-incubated at 25 °C (a) and 50 °C (b).

Figure S4. Flow cytometry analyzed fluorescence intensity of 4T1 cells.

Figure S5. CLSM images of T-lipos-CPAuNCs treated different cells.

Figure S6. Semi-quantitative analysis of COX-2 expression in drugs treated 4T1 cancer cells.

Figure S7. Hemolytic activity of T-lipos-CPAuNCs.

Figure S8. Ex vivo DiD fluorescence images.

Figure S9. Observation of tumor recurrence of mice.

Figure S10. Biochemical index.

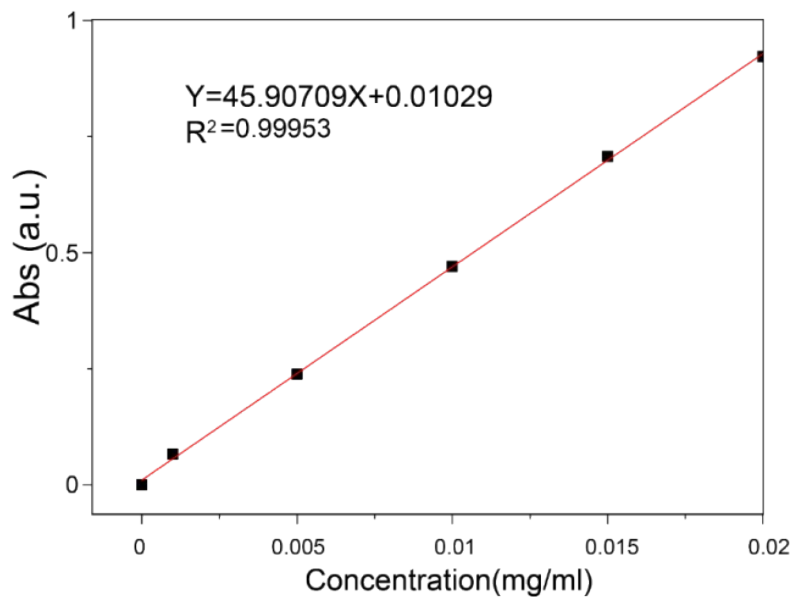


Figure S1. Standard absorption curve of Celecoxib by UV-vis spectrophotometry.

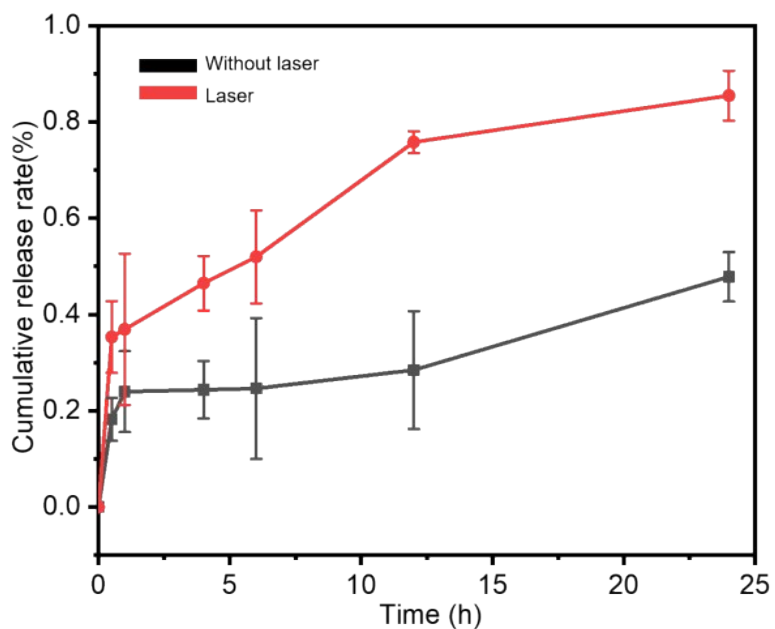


Figure S2. The cumulative release curves of Celecoxib from T-lipos-CPAuNCs with/without laser irradiation (pH 6.5).

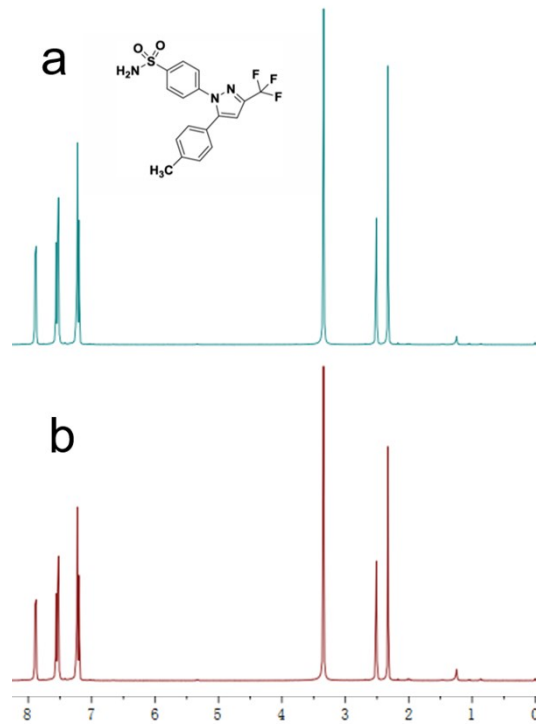


Figure S3. ¹H NMR spectra of Celecoxib pre-incubated at 25 °C (a) and 50 °C (b).

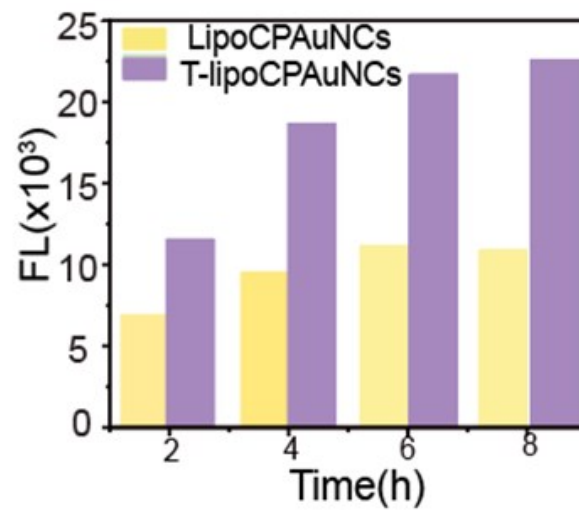


Figure S4. Flow cytometry analysed fluorescence intensity of 4T1 cells after treating with T-lipo-CPAuNCs and Lipo-CPAuNCs (DiD 5 μM Ex: 644 nm, Em: 665 nm)

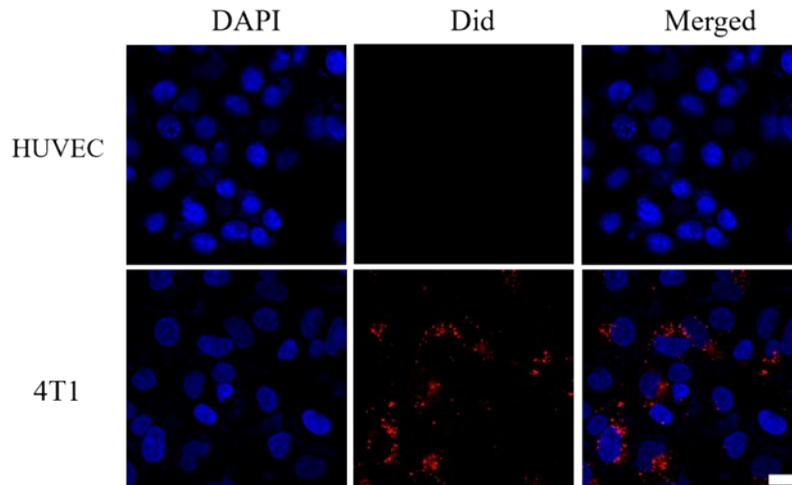


Figure S5. CLSM images of different cells (HUVEC and 4T1 cells) after incubating with DiD contained T-lipos-CPAuNCs (DiD: 5 μ M) for 6 h (the scale bar was 10 μ m).

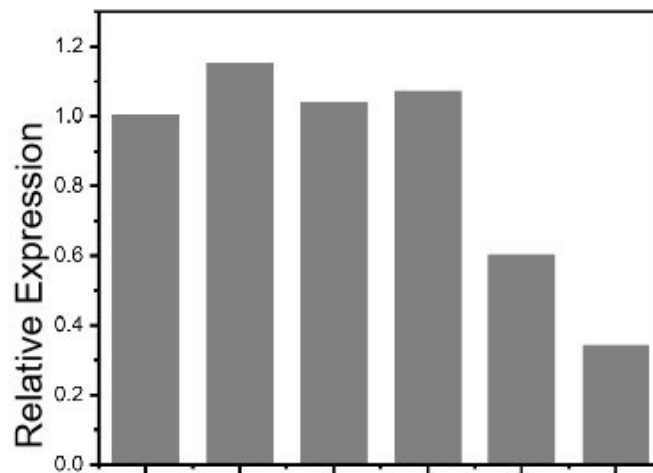


Figure S6. Semi-quantitative analysis of COX-2 expression in drugs treated 4T1 cancer cells determined by Western blot assay (1. PBS+L; 2. T-Lipo-PAuNCs-L; 3. T-Lipo-CPAuNCs-L; 4. T-Lipo-PAuNCs+L; 5. T-Lipo-CPAuNCs+L; 6. Celecoxib).

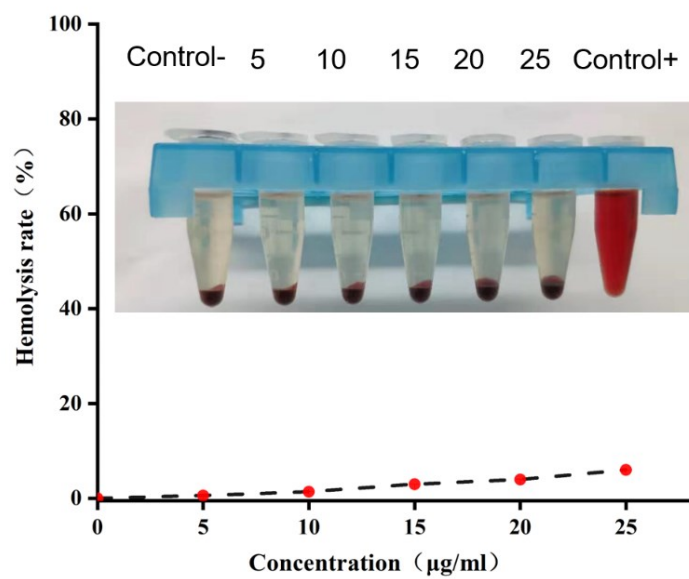


Figure S7. Hemolytic activity of T-lipos-CPAuNCs on rat erythrocytes. T-lipos-CPAuNCs were incubated for 2 h with 2% erythrocytes in phosphate buffer solution, the suspensions were centrifuged, and the absorbance of supernatant (100 µL) was measured at 450 nm.

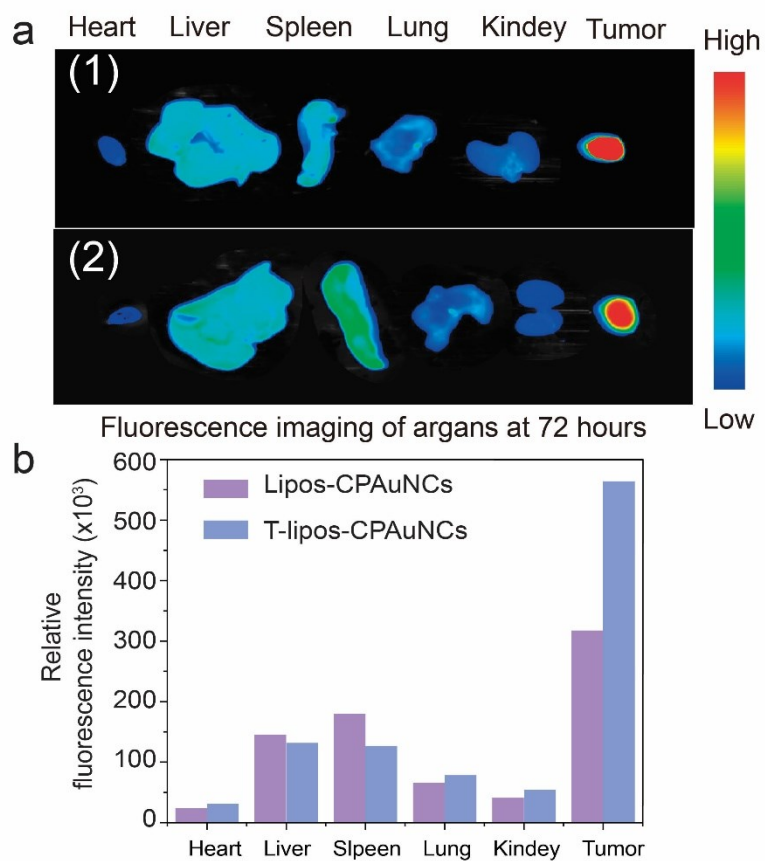


Figure S8. a) Ex vivo DiD fluorescence images showing (1) T-lipos-CPAuNCs, (2) Lipos-CPAuNCs tissue bio-distribution of after 72 h injection; b) Semi-quantitative fluorescence intensity of tissue distributions.

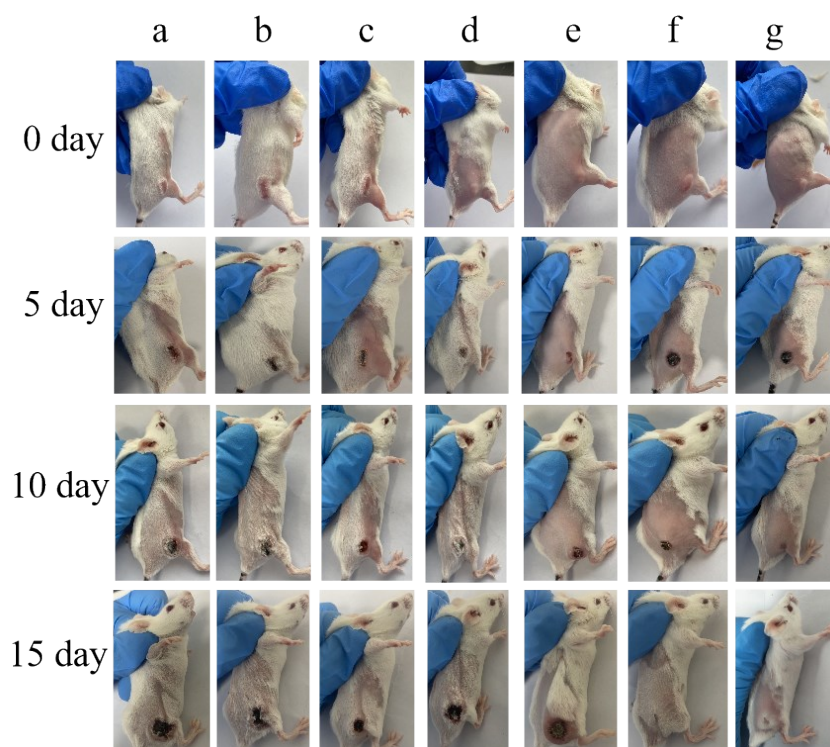


Figure S9. Observation of tumor recurrence of mice after 16 days anti-tumor treatment. a) PBS-laser; b) PBS+laser; c) Cel; d) T-Lipos-CPAuNCs-Laser; e) Lipos-CPAuNCs+laser; f) T-lipos-PAuNCs+laser; g) T-Lipos-CPAuNCs+laser.

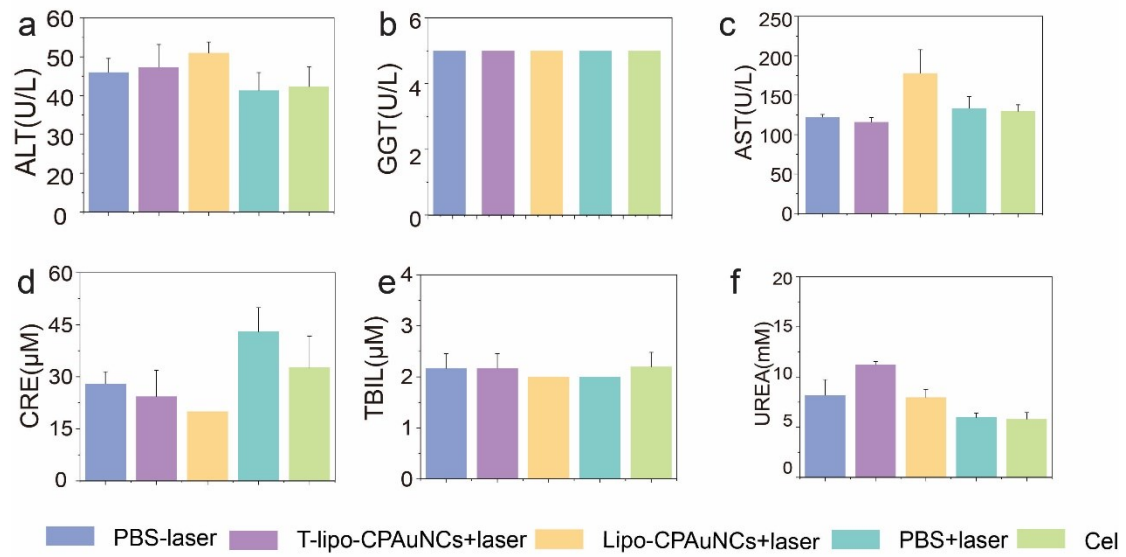


Figure S10. Biochemical index including: a) alanine aminotransferase (ALT), b) glutamyltranspeptidase (GGT), c) aspartateaminotransferase (AST), d) creatinine (CRE), e) total bilirubin (TBIL), f) blood urea nitrogen (UREA), of 4T1 tumor-bearing mice after treating for 15 days. (n=3).